

Solar Array Deployment Mechanism

Mark C. Calassa* and Russell Kackley*

Abstract

This paper describes a Solar Array Deployment Mechanism (SADM) used to deploy a rigid solar array panel on a commercial spacecraft. The application required a deployment mechanism design that was not only lightweight, but also could be produced and installed at the lowest possible cost. This paper covers design, test, and analysis of a mechanism that meets these requirements.

Introduction

Figure 1 shows a sketch of the solar array in its on-orbit, fully deployed configuration. The SADM is used to deploy the solar array panel shown in the figure. The panel is of typical construction, using aluminum face-sheets bonded to an aluminum honeycomb core. During launch, the solar array is stowed against the main structure. Once on orbit, commands are sent to release devices to release the solar array. The SADM provides the torque to rotate the solar array to a prescribed angle and the stop device to hold it in position at the end of deployment.

Design Description

Figure 2 shows the SADM components and their physical interfaces to the adjacent spacecraft structure. The SADM consists of two hinge assemblies, one fixed and one floating, and a foldable semi-lenticular ("C-section") strut. These mechanisms provide torque to rotate each solar array panel from the stowed (launch) configuration to the deployed (functional) position. The solar array deployment is a one-time, passive event that can not be stopped once initiated.

Each hinge assembly has a torsion spring that drives the solar array panel into its deployed position. Figure 3 shows an exploded view of the fixed hinge assembly. Self-lubricated, Teflon-lined journal bearings provide a low-friction rotational joint. Each hinge is rotationally redundant since the hinge pin is free to rotate in both the tang part and the clevis part. A sealed Rotary Viscous Damper (RVD) mounts on the fixed hinge assembly. The RVD was designed to control deployment speed to reduce the solar array panel lock-up loads (at the strut attach point) from 1112 N (250 lb) (undamped) to 600 N (135 lb) (damped) to protect solar array components. A resistive element heater is bonded to the exterior of the RVD to limit cold temperatures to greater than -36 °C. Figure 4 shows an exploded view of the floating hinge assembly. The clevis gap dimension on the floating hinge assembly was sized to accommodate differential thermal expansion between the graphite-epoxy spacecraft structure and the aluminum substrate of the solar array panel. The tang part of the floating hinge

* Lockheed Missiles and Space Company, Inc., Sunnyvale, CA

also incorporates a spherical bearing (monoball) to help prevent hinge binding during deployment.

The stop and alignment strut (shown in Figure 2) is made of 0.305 mm (0.012 in) titanium sheet formed into a C-section with a 38.1 mm (1.5 in) radius of curvature. It is 58.4 mm (2.3 in) wide and 1.3 m (51 in) long. The strut is folded between the spacecraft and the solar array panel when stowed, and provides deployment torque, an end-of-motion stop, and alignment when the solar array panel is fully deployed.

The solar array transfers power to the satellite by means of wire harnesses crossing the hinge axis. The harnesses are located between the fixed and floating hinge. The harnesses include power, grounding, and data cables. Except for the RVD and wire harnesses, all components in the SADM were designed to be insensitive to large temperature variations. All relative rotating surfaces (radial and sliding) have positive clearances even at worst case temperature extremes. The wire harnesses crossing the joint were included in the design and testing because they present the major resistance torque against which the SADM must work.

Requirements

The table below shows the requirements and capabilities matrix for the SADM.

SADM Requirements and Capabilities Matrix

SUBJECT	REQUIREMENT	CAPABILITY	VERIFICATION METHOD
Deployment Time	Less than 7 minutes	5 seconds to 5 minutes	Analysis and test
Deployed Frequency	Greater than 0.5 Hz	Greater than 0.5 Hz	Analysis and test
Mechanical Alignment			
•Azimuth	Less than 0.25°	0.245° max	Analysis
•Elevation	Less than 0.30°	0.204° max	Analysis
Mass (each)	< 1.50 kg (3.3 lbm)	1.23 kg (2.72 lbm)	Analysis
Torque Margin	Greater than 0	1.0 (100%) Minimum	Analysis and test
Thermal	81 °C Max/-64 °C Min 55 °C Max/-36 °C Min for Rotary Viscous Damper	Comply by design	Analysis and test
Reliability	Greater than 0.999	Greater than 0.999999	Analysis
Shelf Life	7 years	Comply	Analysis
Ground Test Life	20 deployments	Comply, more than 50 deployments done	Test

Design Features

The SADM has several interesting design features. These features were required to support the low cost of production and installation goals. The first is the semi-lenticular strut, which provides moderate deployment force, an end-of-travel stop, deployed alignment repeatability, and increased deployed frequency. The strut was selected over other stop and alignment devices because it is compact, lightweight, has high axial stiffness, and does not require complex adjustments to correctly align the solar array. It also acts as a kick-off spring because of energy stored in the flattened section when it is folded. The strut cross-section was selected as a semi-lenticular shape over a closed lenticular shape to minimize manufacturing costs. A fully lenticular strut would have required extensive tooling and inspection for shaping, welding, and heat treating, while the C-section is simply bump formed and then stress relieved. The cost was further reduced by requiring that the C-section radius only be inspected for a 15.2 cm (6 in) zone surrounding the mid-span of the strut radius instead of for the entire 1.3 m (51 in) length. The inspection zone corresponds to the area of the strut where the curved C-section becomes flat when stowed, and the stresses in the titanium reach a maximum. Material thickness, curvature radius, and stowage bend radius, are all critical design parameters influencing the performance of the strut. An extensive development test program was conducted to perform design trades of conflicting parameters such as buckling stability, stowage envelope, deployment torque, and material stress levels. The final design was derived from a careful compromise of these parameters.

A second such design feature is the RVD. The basic RVD design has an extensive flight history with NASA and commercial programs. However, several design improvements were made for the SADM application, as shown in Figure 5. The most significant of these are the change from two fasteners to one (to reduce fastener part count), the unique-sided shaft to prevent improper installation, the fluid fill inspection port, the precision bonded bearings, and the precision pilot boss to provide precise alignment between the hinge axis and the damper shaft. The "indexed" shaft design requires that the damper shaft be in the 0° (stowed) position before installation. This prevents the damper from being installed with the shaft in a deployed position, which would prevent the solar array panels from deploying, thus causing a mission failure. In addition, there is 8° of deadband between the shaft and the hinge shaft boss. The deadband allows easy assembly of the damper into the hinge without worrying about tolerance build-up or the use of an expensive, heavy, coupling design. The fluid fill inspection port enabled the assembly to be inspected for the presence of air bubbles without the costly, time consuming, and sometimes inaccurate, x-ray method. The use of a mandrel type tool to locate and bond bearings into place reduced the major source of variability in damping rate by precisely aligning the vane shaft in the damper case thus reducing leakage past the vanes of the vane shaft.

Finally, most parts of the SADM are aluminum to reduce manufacturing costs.

Testing

An extensive development test program was conducted to verify that all components would function properly before beginning the qualification program. Component tests were performed on the RVD (to determine strength and damping rate), wire harnesses (to determine bending torque), torsion springs (to determine torque output), hinges (to determine friction torque), and the strut (to determine torque output, axial stiffness, and buckling stability). The RVD and wire harnesses were tested at ambient and qualification temperatures (hot and cold).

Figure 6 shows a sketch of the full-scale panel test setup. Since release and lockup loads were important, a full-scale solar array panel was built to simulate the stiffness and inertia of the flight panel. The solar array was simulated by a typical aluminum honeycomb panel design, sized to simultaneously match the bending stiffness and inertia of the actual solar array. This was critical in being able to use the test data to correlate with the analytical model. Flight-quality hinges and struts were used. No attempt was made to use worst-case springs during qual testing. The springs that were used in the qual tests were close to nominal. To account for spring variations, the analytical model was correlated to the test results, and then the model was used to extrapolate to worst-case performance. The hinge line was aligned vertically to eliminate gravity effects on deployment. The test fixture had its own spherical off-load hinges (located outboard of the SADM hinges) to which the panel was attached. Therefore, the off-load hinges supported the full panel weight and prevented the SADM hinges from carrying any gravity-induced side load. The hinge lines of the test stand hinges and the SADM hinges were aligned with tooling to be co-linear. The SADM hinges were mounted to a graphite/epoxy panel on one side, to simulate the thermal expansion characteristics of the spacecraft, and to an aluminum plate on the other side, to simulate the thermal expansion characteristics of the solar array. Full-scale deployment tests were conducted at ambient and at qualification hot/cold temperatures. Figure 7 shows a chamber that was built around the hinge line to facilitate hot and cold development tests. The strut was not expected to be thermally sensitive, so it was left at ambient temperature. Figure 8 shows the solar array panel in the deployed position following a functional test.

The test fixture was equipped with many real-time computer-compatible instruments. A load cell was used between the hinge and the panel to measure the torque required to rotate the panel during the hinge friction and wire harness tests. A rotary potentiometer was used to measure the panel deployment angle. A strain gage bonded onto the RVD shaft was used to measure torque in the RVD. The shaft torque was of concern because of the 8° deadband between the hinge boss and the damper shaft. A load cell in line with the strut was used to measure lock-up load. All torque, angle, and force data were recorded and viewed "real time" on a Macintosh computer running the LabVIEW¹ software. All instrumentation was for the test only; there is no provision for measuring torque or angle during an on-orbit deployment.

¹LabVIEW is a trademark of National Instruments Corporation.

Several important facts were learned about the components as a result of development testing. Some of these led to design changes before qual testing. Figure 9 shows a plot of the wire harness torques. These torques were acceptable and no changes were made to wire harness routing. However, the electrical power group asked that a change be made to the power cables, so it was re-tested and found to be an insignificant change relative to the wire harness torques.

First, it was discovered that the strut was resisting deployment at the end of travel. In the original design, the bending stresses in the bent section when the strut was stowed against the spacecraft were high enough to cause localized yielding at the edges of the strut. This yielding changed the strut output torque characteristics so that it resisted, instead of aided, deployment at the end of travel. This resulted in a negative torque margin and the panel would not deploy properly. The strut thickness was decreased from 0.406 mm (0.016 in) to 0.305 mm (0.012 in) to reduce the peak bending stresses. Reducing the stresses eliminated the yielding and resulted in a strut torque that always aided deployment. Figure 10 shows a plot of the strut output torque before and after the design change. The thinner material reduced the tensile strength and buckling force slightly, but the margins were still acceptable.

Second, the location of the spring mandrel pin on the hinges was changed slightly to wind up the torsion springs by an additional 15° for increased torque output. This was done to increase torque margin without redesigning the springs. The unique design of the spring end and spring mandrel pin allowed a cost effective way to increase torque by re-drilling only one hole. It should be noted that the spring design was initially sized with extra stress margins in case such a design change needed to be implemented. At the same time, the location of the mandrel pin was moved axially along the spring mandrel to reduce the coil-to-coil rubbing on the torsion spring. This reduced the hinge friction as a percentage of the spring torque. It was also found that the MoS₂ dry film (on the springs) was tending to gall and deposit on the soft aluminum of the spring mandrel, thus causing extra resisting torque. The hinge mandrel was subsequently hard anodized to reduce this effect. These changes to the hinge were made quite easily because the hinges were designed to allow changes such as this without major impacts to the design. Figure 11 shows a typical plot of the torsion spring and hinge friction torques before and after the design change.

Finally, it was discovered that the RVD did not rotate when the core temperature was below -40 °C. Initially, the vendor advertised that the RVD would operate at temperatures as low as -54 °C. However, the damper has a steel vane shaft and an aluminum case with very little clearance between the vanes and the case. Due to differential thermal contraction at cold temperatures, the case shrank down onto the vanes and prevented rotation. After this was learned, a heater and thermocouple were added to the RVD to prevent the temperature from going below -36°C before and during deployment. The power consumed by this heater did not significantly affect the spacecraft power budget. After this change, the cold qualification temperature for the RVD was increased from -54 °C to -36 °C. The survival temperature range (-64 °C to 81 °C) was not affected. In addition, it was found that the RVD damping rate was sensitive to both temperature and applied torque, as shown in Figure 12. This did not

adversely affect system performance, but was important to know for analytical performance predictions.

Following the development tests, a qualification test program was completed. Figure 13 shows the test flow. The test stand shown in Figure 6 was placed in a large thermal/vacuum chamber for the hot and cold thermal/vacuum tests. A feed-through was available for connecting the data acquisition system to the sensors on the hardware. Figure 14 shows the deployment time history for the ambient, hot, and cold tests.

All qualification tests were successfully completed and the SADM hardware is now flight qualified.

Analysis

The deployment analysis of the SADM covered two main areas: torque margin and deployment dynamics. Figure 15 shows the torque margin for the qual springs (which produced close to nominal spring torque) and for the worst-case springs. This shows that the margin is above the requirement of zero even for the worst-case springs. A computer simulation of the solar array panel deployment was developed to predict worst-on-worst release and lock-up loads. Figure 16 shows a schematic of the deployment system as it was modeled. The system was modeled using EZDYN, a general purpose, multi-body dynamics analysis code developed at Lockheed Missiles and Space Company. The model included component test data to predict system performance. It also included the capability to create a worst-on-worst combination of parameters to predict maximum loads. The outputs from this model were the following: damper shaft load, deployment time, and lockup loads. Figure 17 shows a typical time history of the panel deployment angle from both test and analysis data. This test data was from the baseline ambient deployment test. The damper shaft load was the critical load for release. The model predicted a worst-case damper shaft load of 50.8 N•m (450 in-lb), compared with a shaft yield capability (from destructive test data) of 112 N•m (990 in-lb). It also predicted a panel lock-up load of 600 N (135 lb). The strut axial strength was tested (destructive test data) to over 7500 N (1700 lb) so it was capable of surviving the maximum lock-up load of even an undamped deployment.

Conclusion and Lessons Learned

A lightweight deployment mechanism applicable to a spacecraft with low cost of production and installation goals has been designed and tested. The mechanism has passed all qualification tests and met all requirements. The following lessons were learned during this process:

- Perform adequate development testing to characterize all components *early* in the test program. Vary as many parameters as possible to get a "gut" feel as to how the mechanism performs and what parameters are really driving its performance.

- **Take the time to characterize individual components of torque or force at temperatures. This alone can save enormous re-qualification costs when hit with last minute design changes. (e.g., introduction of "last minute" cable harnesses)**
- **Don't start out locked into a "point" design. Design components that can easily be upgraded or modified. Keep design options open as long as possible. A design that is on the "hairy" edge during the development phase of a program is probably going to be a "loser."**
- **Don't automatically trust vendor claims of component performance. Test them yourself. Take an early look at potential vendor's test capability and test methods to ensure that they are acceptable for your needs.**
- **Create an analytical model to predict worst-case performance, because one cannot usually test with worst-case components.**

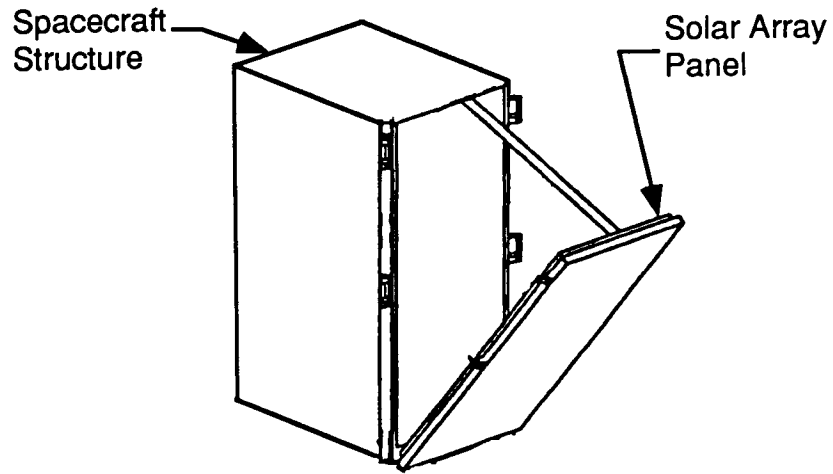


Figure 1. Solar Array in On-Orbit Configuration

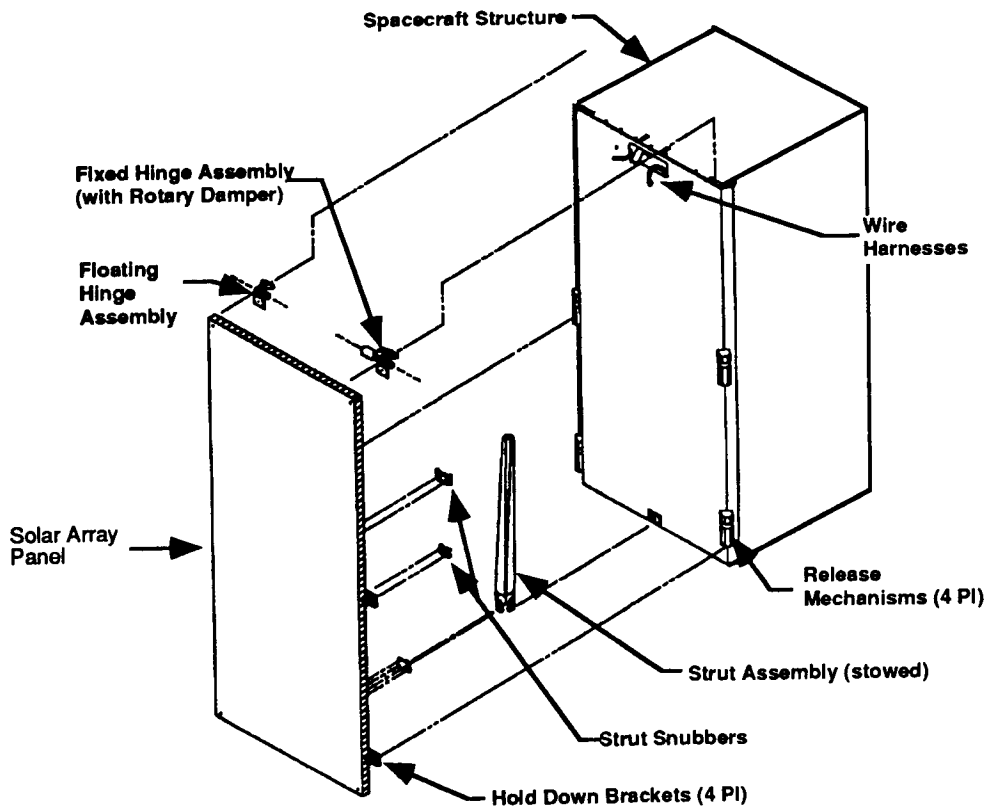


Figure 2. Solar Array Deployment Mechanism Components
 (Note: Drawing is rotated 180° from Figure 1)

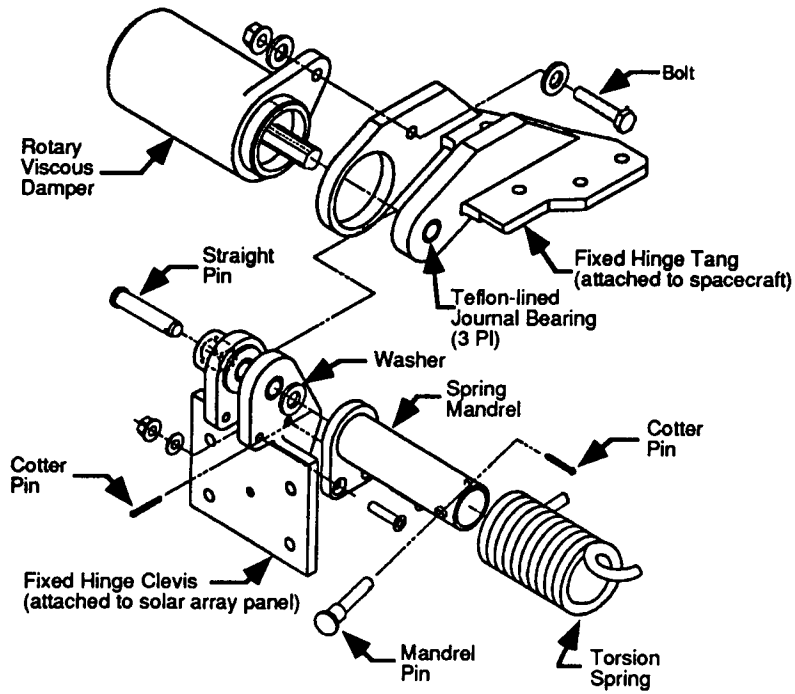


Figure 3. SADM Fixed Hinge Assembly (Stowed Configuration)

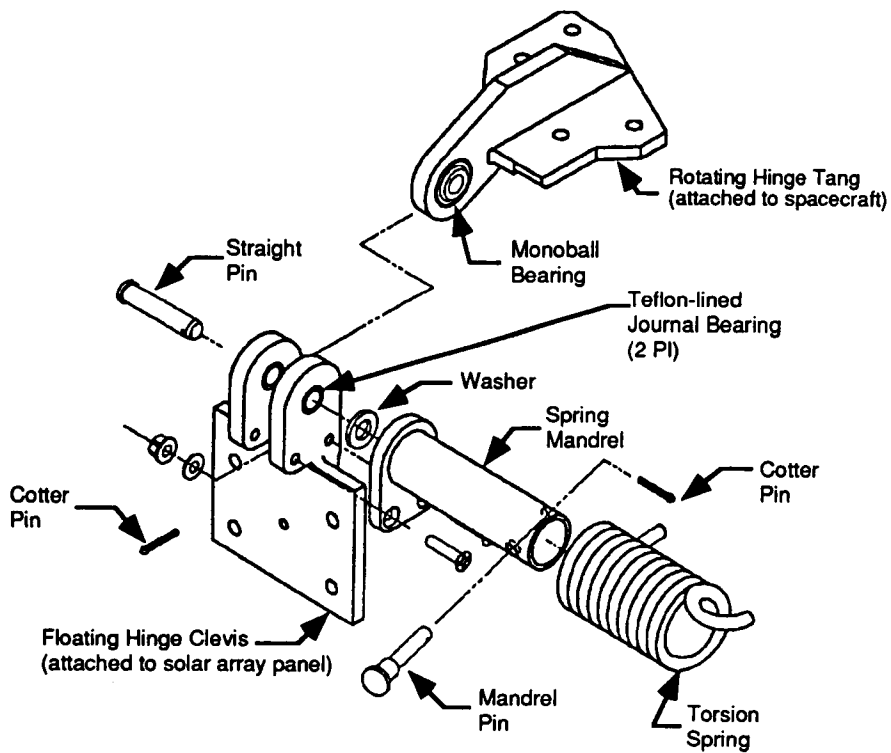


Figure 4. SADM Floating Hinge Assembly (Stowed Configuration)

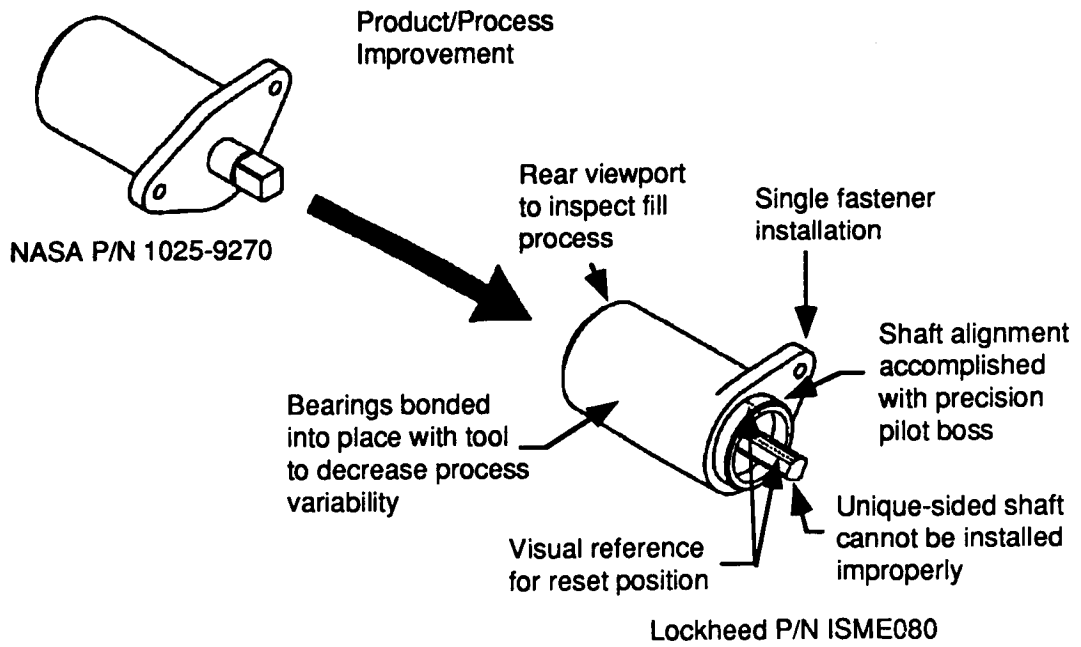


Figure 5. Rotary Viscous Damper Improvements

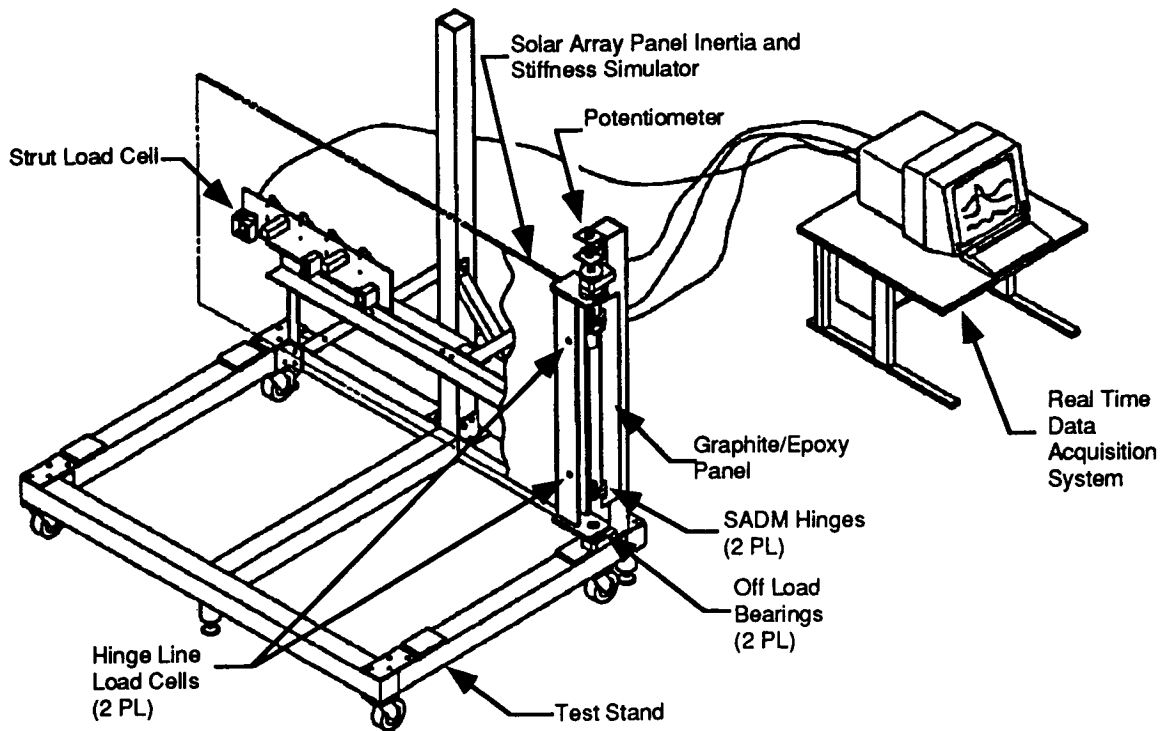


Figure 6. SADM Deployment Test Setup

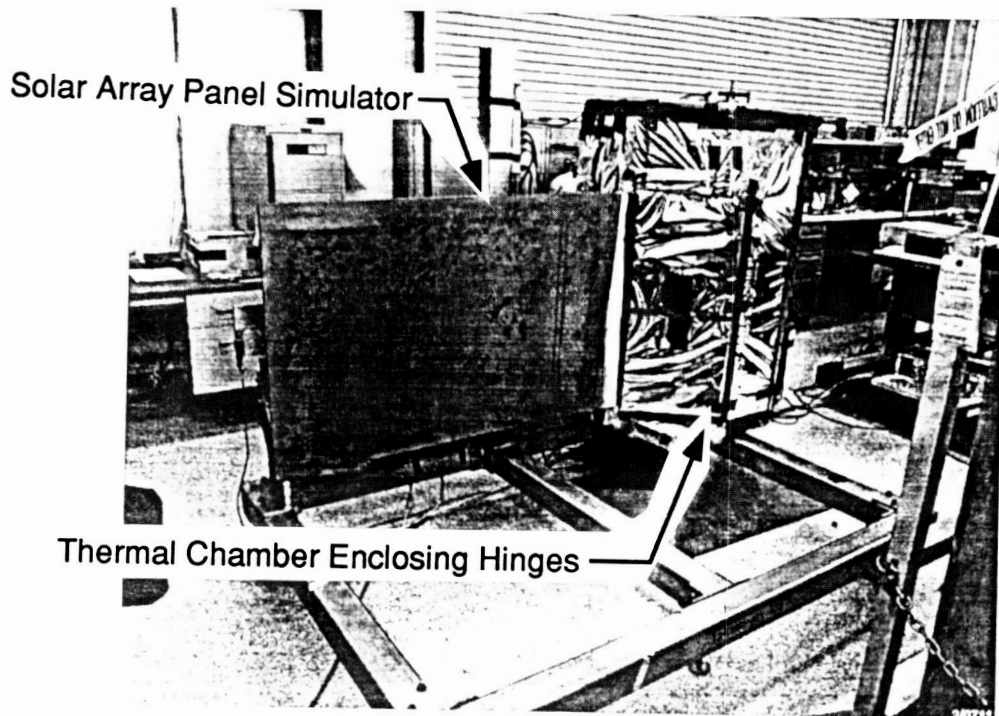


Figure 7. SADM Development Test

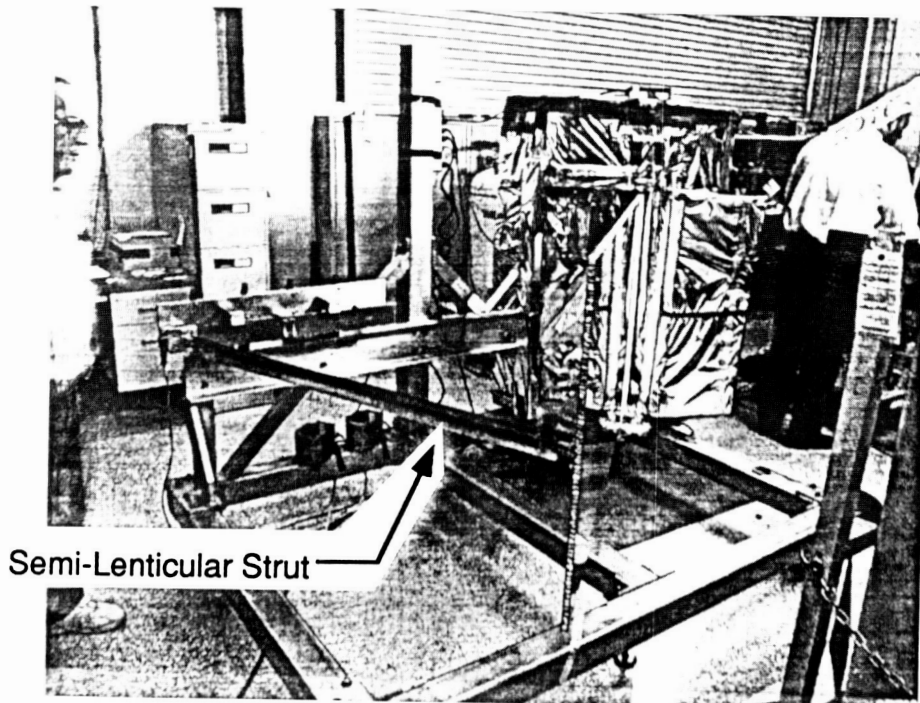


Figure 8. Solar Array Panel in Deployed Position

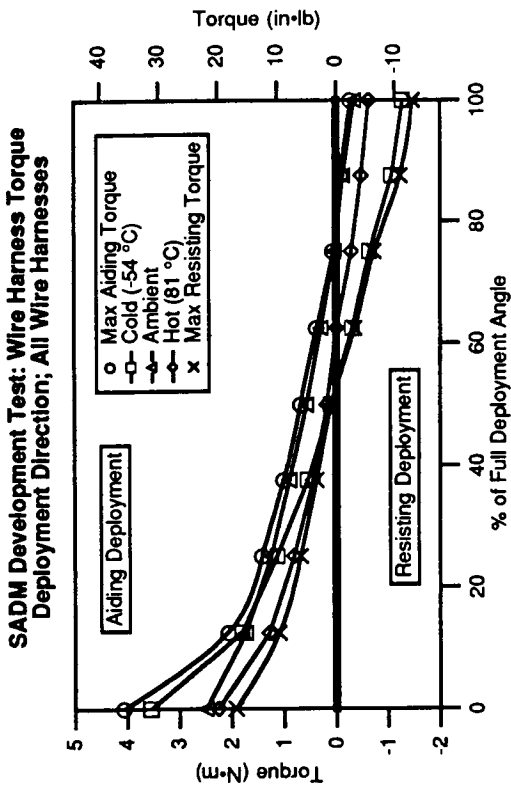


Figure 9. Wire Harness Torque from Development Tests

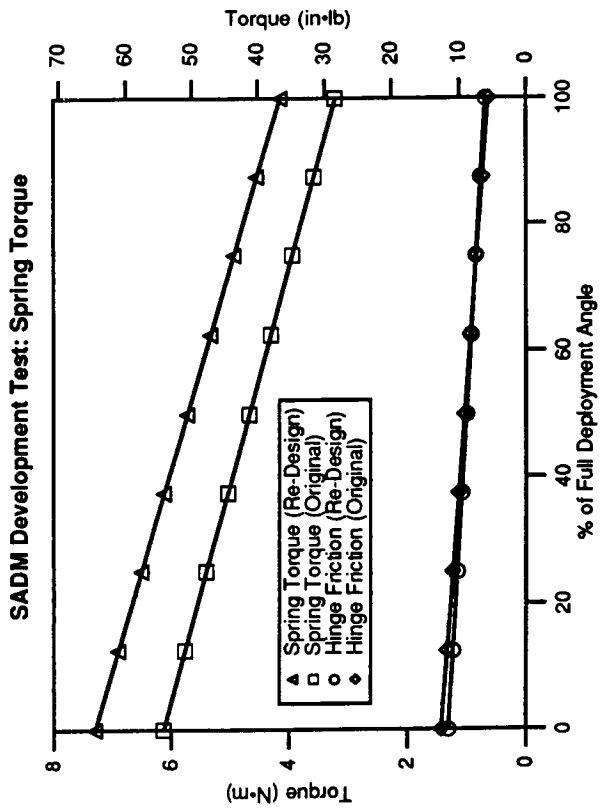


Figure 11. Spring Torque and Hinge Friction

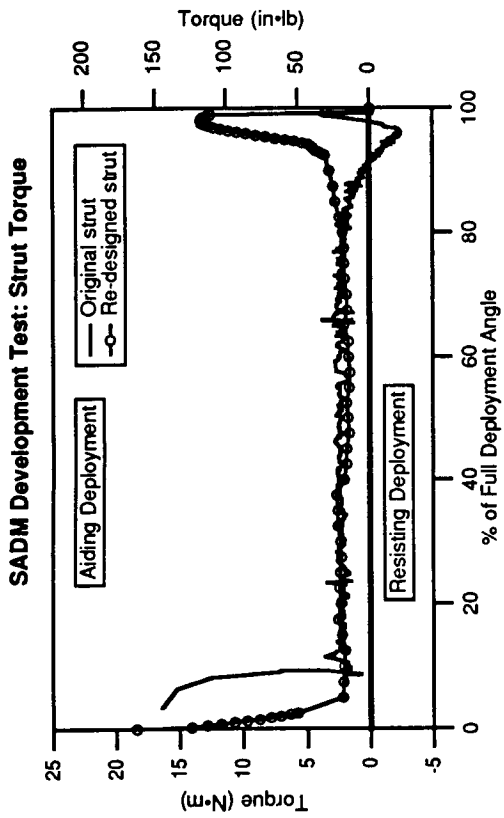


Figure 10. Strut Torque from Development Tests

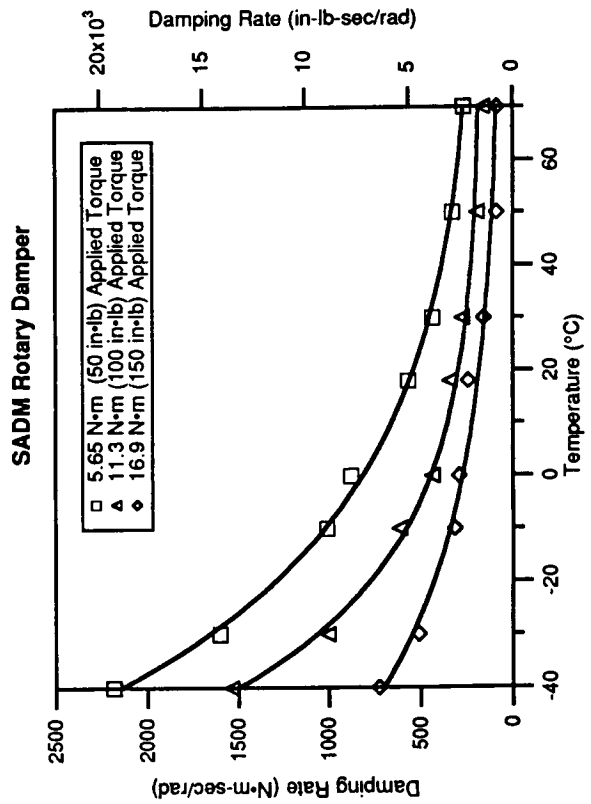


Figure 12. Rotary Damper Characteristics

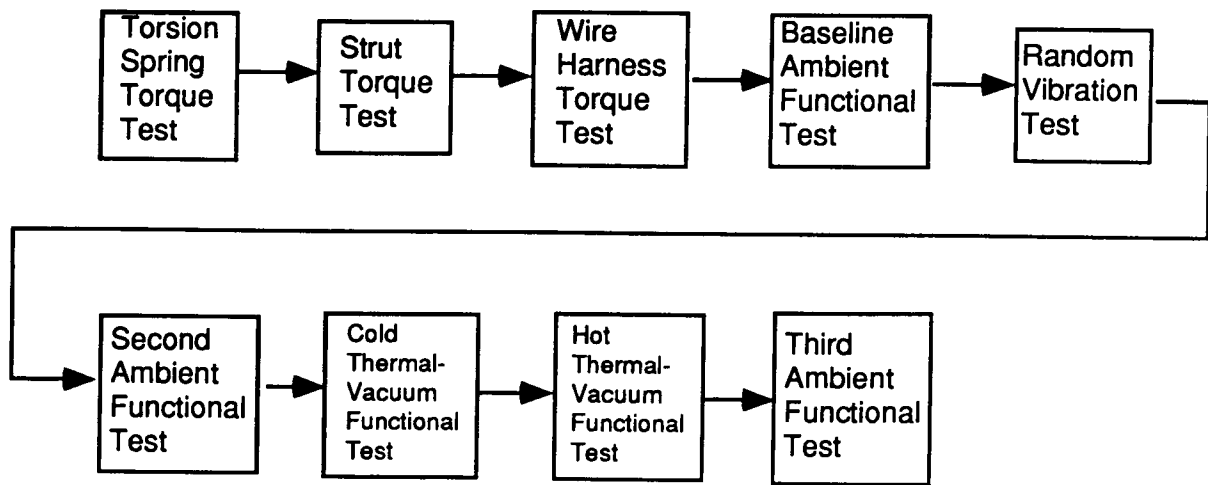


Figure 13. SADM Qualification Test Sequence

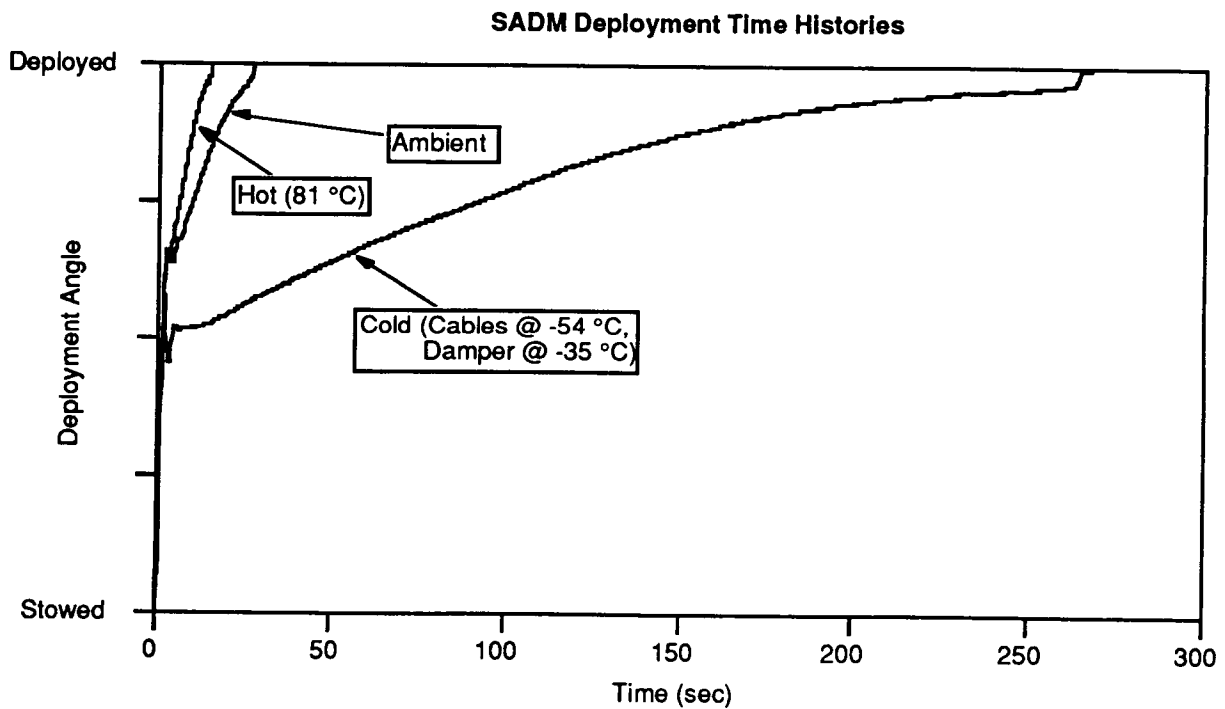


Figure 14. SADM Deployment Test Results

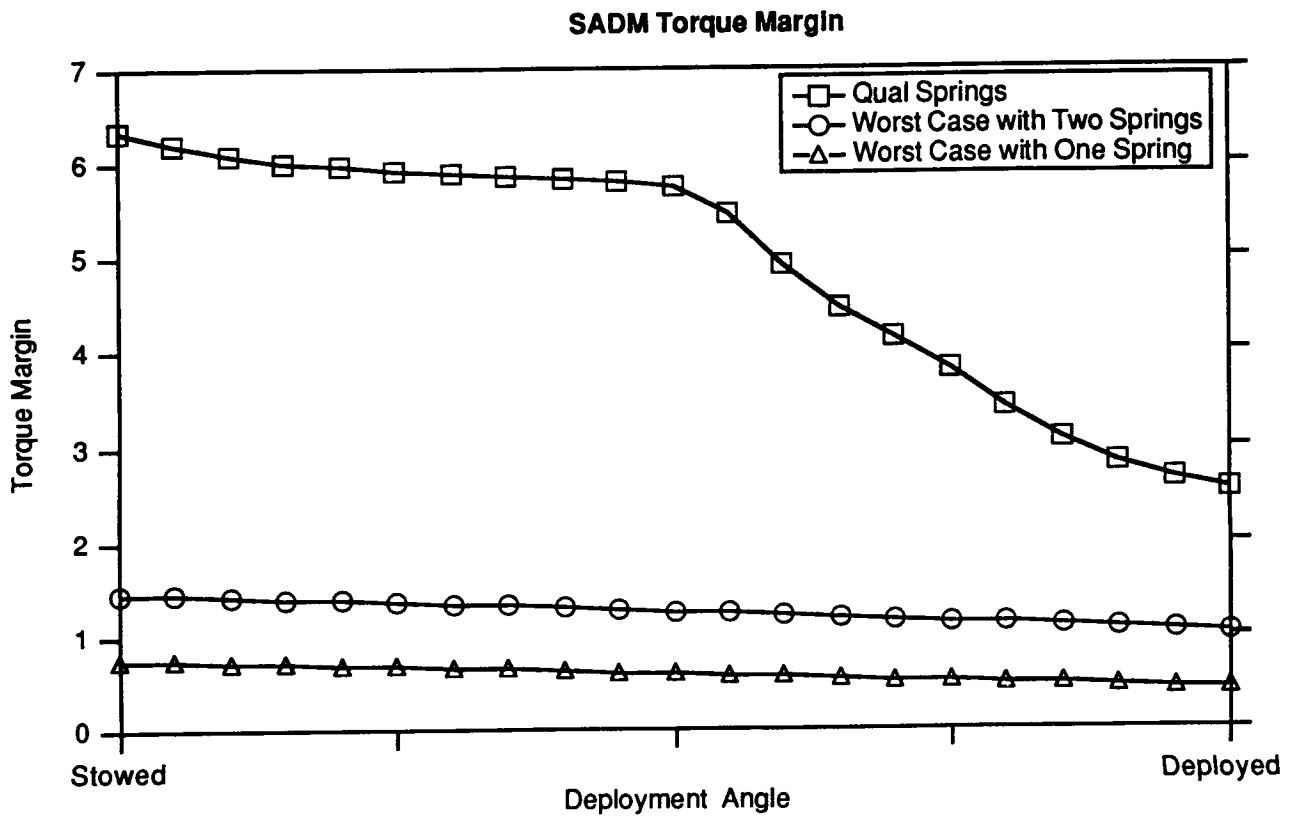


Figure 15. Torque Margin with Qual Hardware and Worst Case Predictions

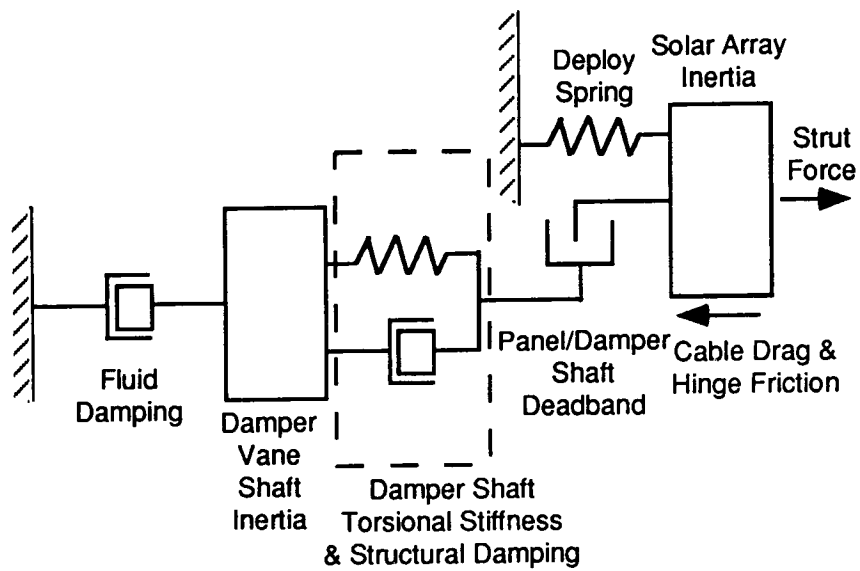


Figure 16. SADM Analytical Deployment Model